

## Table of Contents

	<b>Page</b>
1 Effect of CT Simulator Tube Voltages on CT Number and Relative Electron Density of CT Images  <i>D P De Sliva, A H Dilip Kumara, K L Priyalal, K L I Gunawardhana</i>	04
2 Incorporation of Wood ash and waste glass powder in enhancing concrete block performance  <i>P V T Prarthana, R C L De Silva, P Subramanium, S Thuraisingam, J Prabagar</i>	17
3 Low-Pressure and Atmospheric-Pressure Cold Plasma Treatment as a Pretreatment for Extracting Volatile Oils from Black Pepper ( <i>Piper nigrum</i> ) Seeds  <i>A B G C J De Silva, H D Weerathunge, P N R J Amunugoda, S H P Gunawrdena, A A P de Alwis</i>	25
4 Photocatalytic degradation of methylene blue dye using silver nanoparticles prepared from <i>Raphanus sativus</i>  <i>M Y F Hasna, S Anuluxan, S Prabagar, R C L De Silva, S Thuraisingam, J Prabagar</i>	39

- Frontiers in Physics, 10(May), 1–8. <https://doi.org/10.3389/fphy.2022.895264>
28. Sarangapani, C., Devi, Y., Thirundas, R., Annapure, U. S., & Deshmukh, R. R. (2015). Effect of low-pressure plasma on physico-chemical properties of parboiled rice. *LWT - Food Science and Technology*, 63(1), 452–460. <https://doi.org/10.1016/j.lwt.2015.03.026>
  29. Sarangapani, C., Thirumdas, R., Devi, Y., Trimukhe, A., Deshmukh, R. R., & Annapure, U. S. (2016). Effect of low-pressure plasma on physico-chemical and functional properties of parboiled rice flour. In *Lwt* (Vol. 69). Elsevier Ltd. <https://doi.org/10.1016/j.lwt.2016.02.003>
  30. Schulz, H., Baranska, M., Quilitzsch, R., Schütze, W., & Lösing, G. (2005). Characterization of peppercorn, pepper oil, and pepper oleoresin by vibrational spectroscopy methods. *Journal of Agricultural and Food Chemistry*, 53(9), 3358–3363. <https://doi.org/10.1021/jf048137m>
  31. Setiawan, Y., Prayitnoadi, R. P., & Saputra, E. (2019). Essential oil processing of pepper process with aluminium condenser. *IOP Conference Series: Earth and Environmental Science*, 353(1). <https://doi.org/10.1088/1755-1315/353/1/012060>
  32. Shishir, M. R. I., Karim, N., Bao, T., Gowd, V., Ding, T., Sun, C., & Chen, W. (2020). Cold plasma pretreatment—A novel approach to improve the hot air drying characteristics, kinetic parameters, and nutritional attributes of shiitake mushroom. *Drying Technology*, 38(16), 2134–2150. <https://doi.org/10.1080/07373937.2019.1683860>
  33. Shishpanov, A. I., Bazhin, P. S., Ivanov, D. O., & Meschanov, A. V. (2020). Low-frequency one-electrode discharge in long tubes at low gas pressure. *Plasma Research Express*, 2(1). <https://doi.org/10.1088/2516-1067/ab7e83>
  34. Submitted, A. T., The, F. O. R., Of, D., & Engineering, D. O. F. (2011). Characterization , Comparison and Application of Two Types of Atmospheric Pressure Cold Argon Plasma Jets DOCTOR OF ENGINEERING DEPARTMENT OF PRODUCTION SCIENCE AND GRADUATE SCHOOL OF ENGINEERING.
  35. Tabibian, S. A., Labbafi, M., Askari, G. H., Rezaeinezhad, A. R., & Ghomi, H. (2020). Effect of gliding arc discharge plasma pretreatment on drying kinetic , energy consumption and physico-chemical properties of saffron ( *Crocus sativus* L .). *Journal of Food Engineering*, 270(June 2019), 109766. <https://doi.org/10.1016/j.jfoodeng.2019.109766>
  36. Thirumdas, R., Kadam, D., & Annapure, U. S. (2017a). Cold Plasma : an Alternative Technology for the Starch Modification. *Food Biophysics*. <https://doi.org/10.1007/s11483-017-9468-5>
  37. Thirumdas, R., Kadam, D., & Annapure, U. S. (2017b). Cold Plasma: an Alternative Technology for the Starch Modification. *Food Biophysics*, 12(1), 129–139. <https://doi.org/10.1007/s11483-017-9468-5>
  38. Valencia, A., Laurindo, B., Laroque, D. A., Tiemi, S., Augusto, B., & Carciofi, M. (2022). Cold plasma in food processing: Design , mechanisms , and application. 312(April 2021). <https://doi.org/10.1016/j.jfoodeng.2021.110748>
  39. Yang, X., Cheng, J. H., & Sun, D. W. (2024). Enhancing microorganism inactivation performance through optimization of plate-to-plate dielectric barrier discharge cold plasma reactors. *Food Control*, 157(July 2023), 110164. <https://doi.org/10.1016/j.foodcont.2023.110164>
  40. Yu, H., Zhang, Y., Wong, A., De Rosa, I. M., Chueh, H. S., Grigoriev, M., Williams, T. S., Hsu, T., & Hicks, R. F. (2014). Atmospheric and Vacuum Plasma Treatments of Polymer Surfaces for Enhanced Adhesion in Microelectronics Packaging. *Adhesion in Microelectronics*, 9781118831, 137–172. <https://doi.org/10.1002/9781118831373.ch4>
  41. Ziuzina, D. (2015). ARROW @ TU Dublin Atmospheric Cold Plasma as a Tool for Microbiological Control. 0–258. <https://doi.org/10.21427/D7FW2Z>

**Photocatalytic degradation of methylene blue dye using silver nanoparticles prepared from  
*Raphanus sativus***

M Y F Hasna<sup>1</sup>, S Anuluxan<sup>1</sup>, S Prabagar<sup>2</sup>, R C L De Silva<sup>2</sup>, S Thuraisingam<sup>3</sup>, J Prabagar<sup>\*1</sup>

<sup>1</sup>Department of Chemistry, University of Jaffna, Sri Lanka.

<sup>2</sup>Industrial Technology Institute, Colombo, Sri Lanka.

<sup>3</sup>Palmyrah Research Institute, Sri Lanka

**ABSTRACT**

Green synthesis of silver nanoparticles possesses many merits compared to that of chemical synthetic methods. Silver nanoparticles have been widely used in many applications such as catalytic activity, dye degradation, antimicrobial and anti-inflammatory activities. In this study silver nanoparticles (AgNps) were synthesized using extract of *Raphanus sativus* roots and identified by the UV-Visible spectrophotometer. XRD peaks of the crystal confirmed the face-centered cubic silver crystals with size of 49.16 nm. FT-IR spectrum indicated the functional groups on this nanoparticles. Scanning electron microscope images showed the spherical shapes and size of the AgNps. The photocatalytic degradation of methylene blue was performed by altering the weight of silver nanoparticles and moles of NaBH<sub>4</sub>. The degradation mixtures of 5 mg AgNps and 5 mL of NaBH<sub>4</sub>, 10 mg AgNps and 5 mL of NaBH<sub>4</sub> and 10 mg AgNps and 10 mL of NaBH<sub>4</sub> attain degradation of 5.088%, 83.86 % and 48.067% of the methylene blue respectively. This study revealed that green synthesized silver nanoparticles from the extract of *Raphanus sativus* can act as a photocatalytic dye degradation agent against methylene blue.

**Key words:** Green synthesis, AgNPs, XRD, dye degradation, methylene blue

## INTRODUCTION

Environmental pollution is one of the major problems currently the world is facing. Among other pollutions, water pollution is an urgent crisis as flora and fauna depend on the water for their survival. Industries including textile and apparel use of large quantities of water for fabric processing and coloring. Organic dyes are being used for the coloring of textile products. Dye molecules consist of two components namely the chromophores and auxochromes. The chromophores are mainly responsible for production of color (Gupta, 2009). There are several dyes used in the industries such as basic, acidic, reactive, azo, mordant, vat, disperse and sulfur dyes (Demirbas et al., 2009). The major types of dyes used in the industries are also said to be azo derivative dyes (Forgacs et al., 2004).

Cationic, anionic and nonionic dyes are another way of classification among the dyes (Salleh et al., 2011). Methylene blue is classified under cationic dye and has been widely used in the apparel industry and acute exposure can lead to cyanosis, quadriplegia, necrosis and vomiting (Vadivelan et al., 2005). So, these dyes should be removed from the industrial effluents before it is released into the environment. Several methods have been used for the treatment of wastewater containing organic dyes namely incineration (Lee et al., 2001), biological treatment (García-Montaña et al., 2008), ozonation (Chu et al., 2000) and adoption on solid phases (Prado et al., 2003). But these processes have the following drawbacks: the incineration can produce toxic byproducts, biological treatment takes a long time and bad odor and the ozonation have a short half-life and the stability of ozone is affected by the pH, temperature and presence of salts (Chekir et al., 2016). The heterogeneous photocatalysis becomes a suitable treatment for the organic dye degradation. Many catalysts have been widely used to degrade the dye molecules such as  $\text{TiO}_2$  (Hadei et al., Khasawneh et al., 2021), ZnO (Ahmad et al., Nguyen et al., 2021), silver nanoparticles (Seerangaraj et al., Sharma et al., 2021), grapheme (Wang et al., 2021), graphene oxide (Zhang et al., 2021) and reduced graphene oxide (Bibi et al., 2019).

Nanotechnology is the hot topic in science which is focusing on the synthesis of nano size materials and their applications across all field of science including synthetic and biological chemistry (Fakhari et al., 2019). Nanoparticles comprises of novel chemical, physical and biological properties due to their size and large surface with free dangling bonds which results in higher reactivity when compared to that of bulk materials (Sharma et al., 2020). Silver nanoparticles are being widely used in many applications such as antibacterial (Thi Lan Huong & Nguyen et al., 2021; Anuluxan et al., 2022), antifungal (Mallmann et al., 2015), anti-inflammatory (Jain et al., 2019), and photocatalytic activities (Chand et al., 2021) due to its merits such as ecofriendly, nonallergic, nonirritant and heat resistant nature as well as chemically stable nature (Miri et al., 2018).

Many synthetic methods are available to produce silver nanoparticles such as chemical reduction, light assisted methods, electrochemical methods, and green synthetic method (Pacioni et al., 2015). Green synthetic method is an environmentally friendly method that involves the plant material, fungi or bacteria for the reduction of silver ions to metallic silver. This method has been widely investigated because of its non-toxicity and the usage of low amount of chemicals. Many plant materials have been used form silver nanoparticles such as Turmeric (Alsammarrarie et al., 2018), *Turbinaria ornata* (Anuluxan et al., 2022), *Diospyros lotus* (Hamedi et al., 2019), *Berberis vulgaris* (Behravan et al., 2019), and *Lysiloma acapulcensis* (Garibo et al., 2020). Plant parts contain

primary and secondary metabolites which reduces and stabilizes the formed nano-particles (Irshad et al., 2021). The study reported that *Raphanus sativus* has consist of many biologically active compounds such as flavonoids, phenols, terpenes, glucosinolate and fatty acids (Gamba et al., 2021). Therefore, this research focused on the synthesis of silver nanoparticles using *Raphanus sativus* root and photocatalytic activity of prepared silver nanoparticles was evaluated by the methylene blue (MB) degradation exposed to light irradiation. The effect of experimental conditions, such as amount of catalyst and concentration of  $\text{NaBH}_4$  were studied.

## METHODOLOGY

### Preparation of Silver nanoparticles

Roots of *Raphanus sativus* were washed in deionized water and then the skins were removed from the roots and cut into small pieces. It was shadow dried for 7 days and grounded into powder and stored at room temperature. 5 g of *Raphanus sativus* (Figure 1) powder was added to 100 mL of deionized water and heated at  $70^\circ\text{C}$  for 20 minutes. Then the aqueous solution was filtered and filtrate was stored in a refrigerator at  $4^\circ\text{C}$ .



Figure 2: Dried root sample of *Raphanus sativus*

10 mL of aqueous extract was taken in a conical flask and covered with aluminum foil. Then the aqueous extract was added with 90 mL of 5 mM  $\text{AgNO}_3$ . Solution pH was maintained at 3, 5, 7, 9, and 11. Reaction mixtures were stirred in a shaker for 24 hours at 300 rpm (Fadel and Al-Mashhedy, 2017). It was stored at room temperature until further analysis.

### Characterization of AgNps

The silver nanoparticles were characterized with the UV-Visible spectrophotometer (Jasco V-570 UV/VIS/NIR) with 200 nm to 800 nm scanning range. The phase purity and the crystallinity of silver nanoparticles were analyzed by powder X-ray diffraction (XRD) (PANalytical-AERIS). The XRD pattern was obtained with  $\text{Cu K}\alpha$  radiation ( $\lambda=1.5408 \text{ \AA}$ ) at room temperature, with the operational conditions of accelerated voltage 40 kV and emission current of 44mA. The crystalline size of the nanoparticles was calculated using Scherrer equation,

$$D = \frac{K\lambda}{\beta \cos\theta} \quad (1)$$

Where K – Scherrer constant,  $\lambda$  – X-ray wavelength,  $\beta$  – the line broadening at half the maximum intensity,  $\theta$  – Bragg's angle and D – crystalline size. M Y F Hasna et al., JSLAAS, Vol. 6, Issue 1 (2024) 39-49 by Hitachi SU6600 FE-SEM (Field Emission Scanning Electron Microscope) using carbon tapes.

## Evaluation of photo catalytic degradation of methylene blue

Green synthesized 5 mg of AgNps and 5 mL of 1mM NaBH<sub>4</sub> were added into 50 mL methylene blue solution (10 ppm). A control was prepared in a similar manner without addition of AgNps. The mixtures were stirred under dark condition for 30 minutes to attain equilibrium. Then the mixtures were kept under light irradiation with stirring until its complete decolorized and the samples were withdrawn at 30 minutes interval and analyzed with UV-Vis spectrophotometer (Arunachalam et al., 2012). The following parameters were chosen to obtain the optimum condition for the photocatalytic degradation; 5 mg of AgNps and 5 mL of 1 mM NaBH<sub>4</sub> (a), 10 mg of AgNps and 5mL of 1mM NaBH<sub>4</sub> (b), and 10 mg of AgNps and 10mL of 1mM NaBH<sub>4</sub> (c). The degradation percentage was calculated by the following equation.

$$R = \frac{(C_0 - C_t)}{C_0} \times 100\%$$

## RESULTS AND DISCUSSION

### Characterization of silver nano-particles

The colour change from yellow to dark brown were observed after the incubation period from the shaker which is due to the reduction of Ag<sup>+</sup> ion to Ag metallic nanoparticles. The production of nanoparticles was checked at various pH using UV-Visible spectrophotometer. As shown in the figure 2, UV-Visible peak at 430 nm confirmed the AgNps formation and the highest intensity peak was observed at pH 9 and the lowest peak was observed at pH 7. The formation of peaks around the 430 nm are due to surface plasmon resonance effect which is caused by the excitation of the electrons and passed to the conduction band of nanoparticles (Gul et al, 2016). The figure 3 shows that the colour became intense with the increase of pH

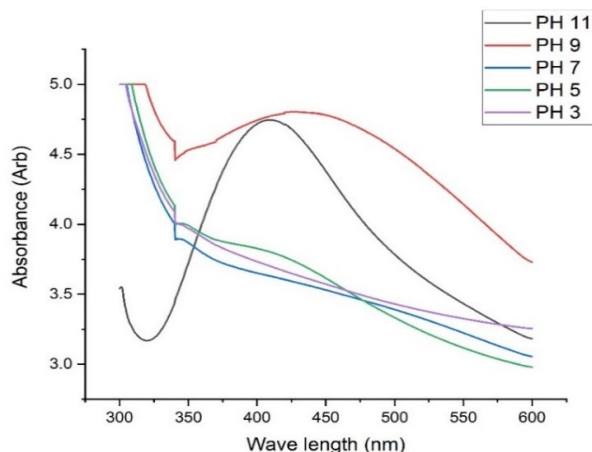
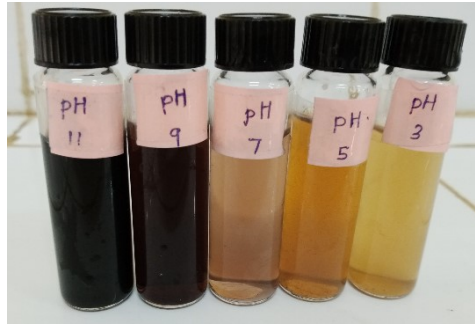
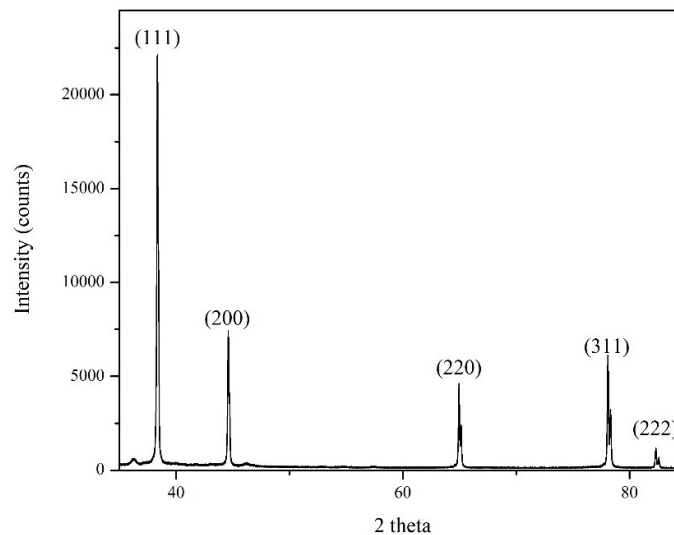


Figure 3: UV-Visible spectrum of synthesized AgNps at different pH



**Figure 4:** Colour of the AgNps mixture after 24 hours of incubation period

The crystalline nature of the synthesized AgNps was analyzed using X-ray crystallography. Figure 4 clearly shows the pattern of synthesized AgNps and main peaks of  $38.32^\circ$ ,  $44.59^\circ$ ,  $64.91^\circ$ ,  $78.16^\circ$  and  $82.44^\circ$  corresponds to the planes of (111), (200), (220), (311), and (222) respectively. These planes confirmed the face-centered cubic silver crystals. The nanoparticle size was found to be 49.16 nm which indicate green synthesized AgNps falls under nanoparticle range.



**Figure 5:** XRD Spectrum of synthesized AgNps

FT-IR spectroscopic technique contributes significantly in the identification of the functional groups which are present in the plant extract. The functional groups are responsible for the reduction of silver ions from silver nitrate and stabilized the synthesized AgNps. FT-IR spectrum of the synthesized AgNps is shown in Figure 5. The absorption peak at  $1347\text{cm}^{-1}$  was assigned to the C-H bending frequency of alkane and  $1037\text{cm}^{-1}$  is due to the C-C stretching frequency of alkane. The peak at  $1590\text{cm}^{-1}$  was arisen due to the bending frequency of N-H bond of primary amines and the peak at  $3280\text{cm}^{-1}$  corresponds to the stretching frequency of the O-H bond of hydroxyl groups. Protein molecules could be present in the plant extract and act as a stabilizing and reducing agent. Gole *et al.* (2001) mentioned that the cysteine from the protein molecules can bind to the AgNps and prevent aggregation by functioning as the capping or stabilizing agent. Gamba, *etal* (2021) reported that the sprout of *Raphanus sativus* contains glucosinolates, flavonoids,  $\beta$ -carotene.

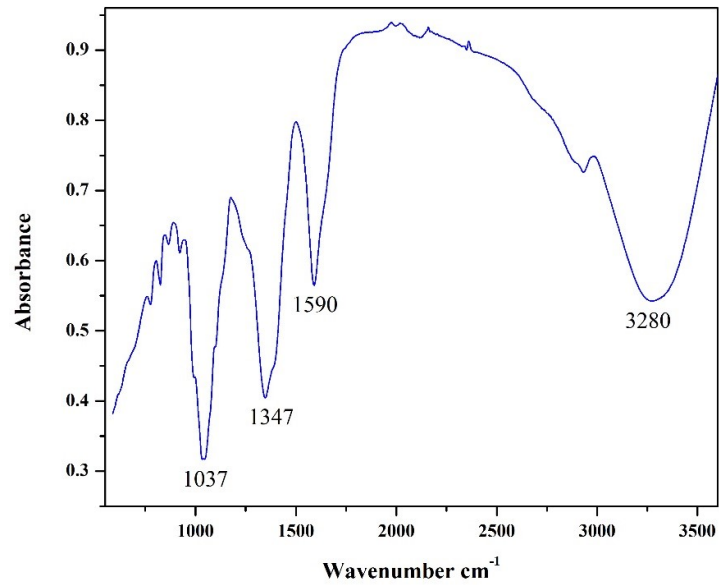


**Figure 6:** FT-IR spectrum of AgNps

SEM images show the surface morphology of the AgNps and most of the synthesized nanoparticles were found in spherical shapes (Figure 6). SEM images of the nanoparticles revealed that the nanoparticles were found in size below 100 nm.

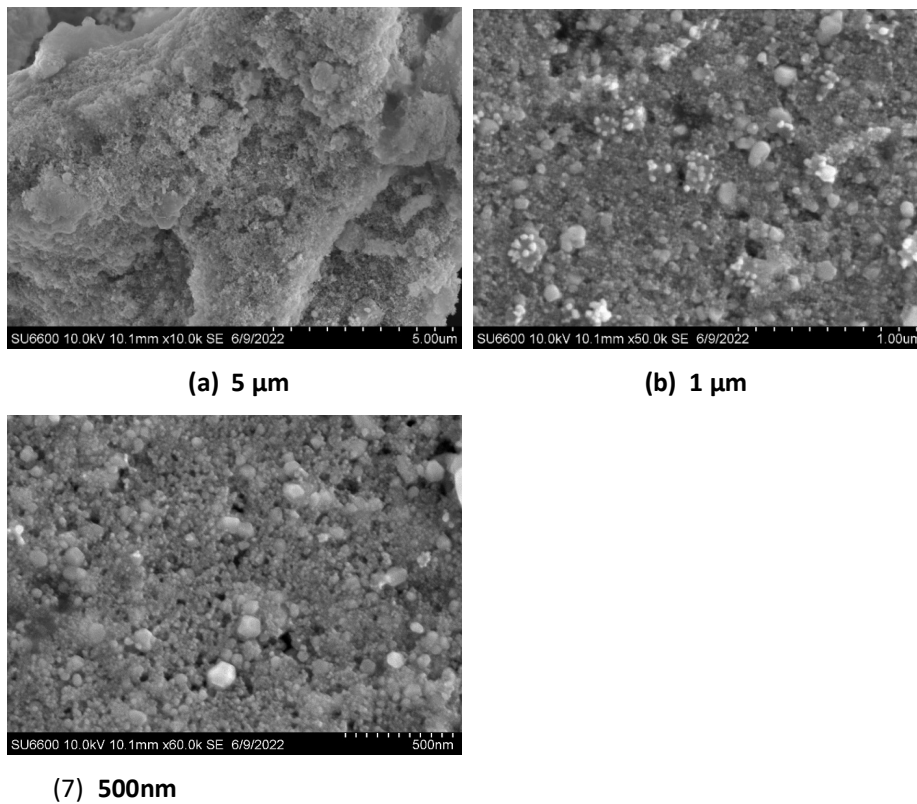


**Figure 7:** SEM images of synthesized AgNPs



**Photo catalytic degradation of methylene blue**

Figure 7 a-c shows the photo catalytic degradation of methylene blue where the parameters such as weight of AgNps and NaBH<sub>4</sub> were altered. Maximum absorbance of MB was observed in UV/Visible spectrometer at 670 nm. The effect of initial concentration of AgNps under light source was studied by using two different concentrations of the initial AgNps (5 and 10 mg per 50 mL) with 10 mgL<sup>-1</sup> concentration of MB dye as shown in Figures 7a and 7b. The rate of degradation was found to be 5.088 % at 240 minutes with 5 mg AgNps and 5 mL of NaBH<sub>4</sub> and with 10 mg AgNps and 5 mL of NaBH<sub>4</sub> attained 83.86 % at 45 minutes. When concentration of AgNps was increased from 5 to 10 mg, the photo catalytic activity was found to be increasing, this is due to the higher number of active sites on the catalyst. But the degradation rate decreased with NaBH<sub>4</sub> concentration (Figures 7c). The rate of degradation was found to be 48.067 % at 45 minutes with 10 mg AgNps and 10 mL of NaBH<sub>4</sub>. The results indicate that 10 mg AgNps and 5 mL of NaBH<sub>4</sub> are the most active concentration in the degradation of methylene blue dye.

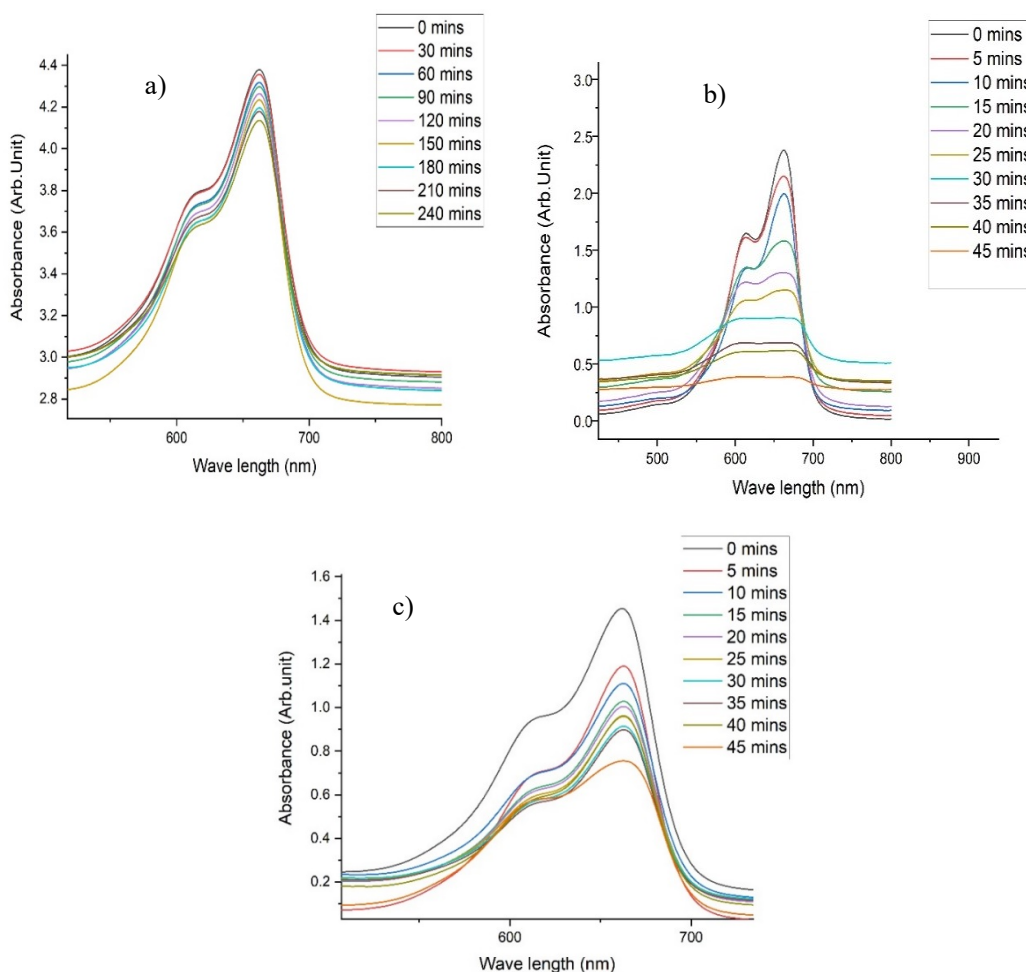


**Figure 8:** UV Vis spectrum of (a) 5 mg AgNps + 5 mL NaBH<sub>4</sub>) (b) 10 mg AgNps + 5 mL NaBH<sub>4</sub>) (c) 10 mg AgNps + 10 mL NaBH<sub>4</sub>)

The rate of photocatalytic degradation of MB was shown in the plot of  $\ln(C/C_0)$  versus time,  $t$  at different experiments a, b and c, (Figures 8a-c).

$$\ln \frac{C}{C_0} = -kt \tag{2}$$

where,  $C_0$  is the initial concentrations of MB in solution and  $C$  is the concentration at times  $t$ , and  $k$  is the first-order rate constant. The kinetics study (Figure 8 a-c) reveals that the MB degradation belongs to first-order kinetics and the rate constants are  $2.26536 \times 10^{-4}$ ,  $0.03912$  and  $0.00923$  for degradation mixtures a, b and c while correlation constants  $R^2$ , for the fitted lines were  $0.97973$ ,  $0.97065$ , and  $0.91637$  respectively.

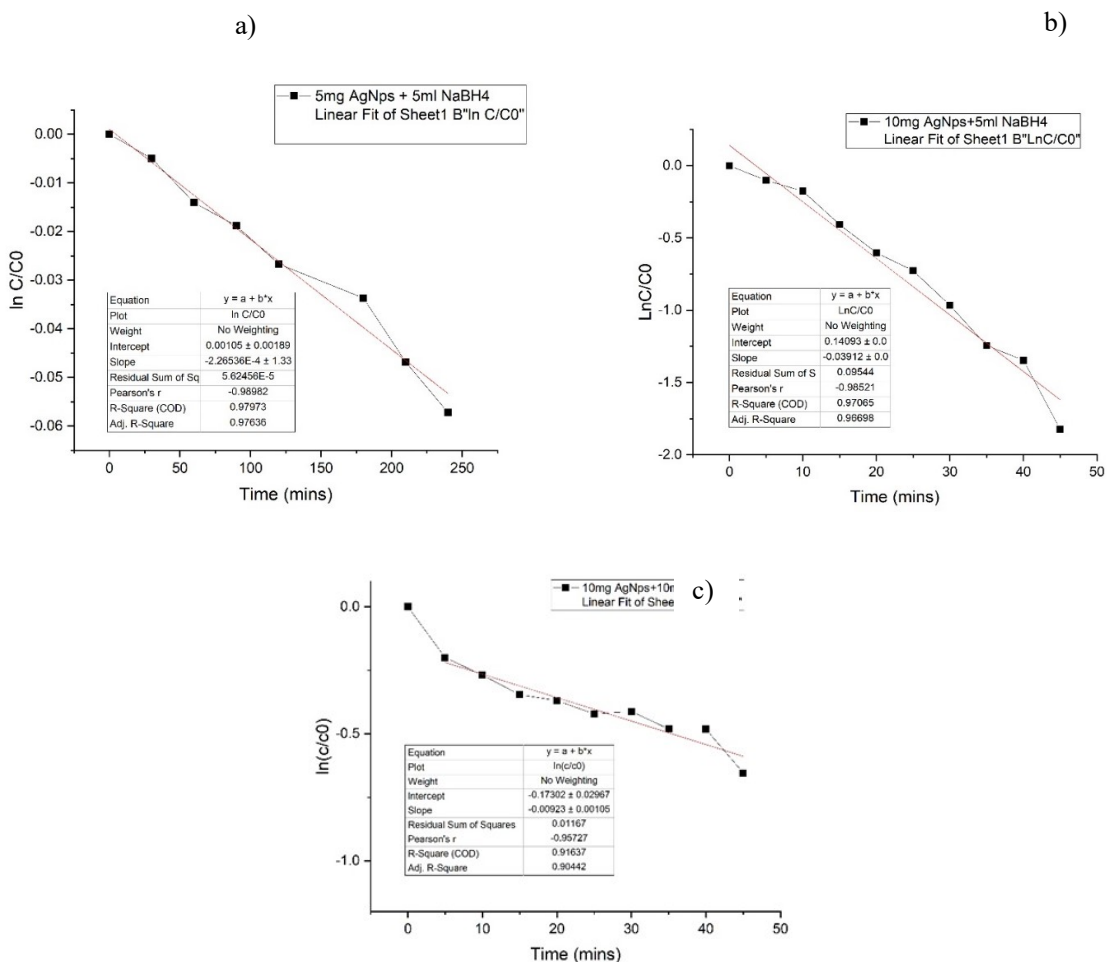


**Figure 9:** Kinetic study of photocatalytic degradation of methylene blue a) 5 mg Ag, 5 mL NaBH<sub>4</sub>, b) 10 mg Ag, 5 mL NaBH<sub>4</sub>, c) 10 mg Ag, 10 mL NaBH<sub>4</sub>

**CONCLUSION**

Silver nanoparticles have been successfully synthesized from the aqueous extract of the *Raphanus sativus* root sample and their performance toward the degradation of hazardous organic dyes was studied. The UV-Visible peak found at 430 nm shows the formation of AgNps. XRD pattern of the

AgNps reveals that the green synthesized AgNps were the face-centered cubic silver crystals. The crystallite size of the synthesized nanoparticles was 49.16 nm. FT-IR spectram confirms the presence of functional groups such as primary amines, free hydroxyl alcohol and phenol which can be due to the presence of protein molecules in the plant extract of *Raphanus sativus*. The degradation of MB dye was performed and a higher percentage of degradation was achieved with mixtures of 10 mg AgNps and 5 mL of NaBH<sub>4</sub>. Biosynthesized AgNps can be effectively utilized to degrade various environmentally hazardous organic dyes.

#### ACKNOWLEDGMENTS

The authors thank the Royal Norwegian Embassy in Sri Lanka for the donation of XRD under capacity building and establishment of research consortium project (Number LKA – 3182 – HRNCET) and AHEAD, ELTA-ELSE Development Project, Department of Chemistry, University of Jaffna for the provision of SEM spectra of the AgNps.

#### FUNDING

This research did not receive any specific grant from funding agencies.

#### REFERENCES

1. Ahmad, M.; Rehman, W.; Khan, M. M.; Qureshi, M. T.; Gul, A.; Haq, S.; Ullah, R.; Rab, A.; Mena, F. J. J. o. E. C. E., Phytogenic fabrication of ZnO and gold decorated ZnO nanoparticles for photocatalytic degradation of Rhodamine B. *Journal of Environmental Chemical Engineering* **2021**, *9* (1), 104725.
2. Alsammarraie, F. K.; Wang, W.; Zhou, P.; Mustapha, A.; Lin, M. J. C.; Biointerfaces, S. B., Green synthesis of silver nanoparticles using turmeric extracts and investigation of their antibacterial activities. *Colloids and Surfaces B: Biointerfaces* **2018**, *171*, 398-405.
3. Anuluxan, S.; Thavaranjit, A.; Prabagar, S.; De Silva, R.; Prabagar, J. J. C. P., Synthesis of silver nanoparticles from *Turbinaria ornata* and its antibacterial activity against water contaminating bacteria. *Chemical Papers* **2022**, *76* (4), 2365-2374.
4. Arunachalam, R.; Dhanasingh, S.; Kalimuthu, B.; Uthirappan, M.; Rose, C.; Mandal, A. B., Phytosynthesis of silver nanoparticles using *Coccinia grandis* leaf extract and its application in the photocatalytic degradation. *Colloids and surfaces. B, Biointerfaces* **2012**, *94*, 226-30.
5. Behravan, M.; Panahi, A. H.; Naghizadeh, A.; Ziaee, M.; Mahdavi, R.; Mirzapour, A. J. I. j. o. b. m., Facile green synthesis of silver nanoparticles using *Berberis vulgaris* leaf and root aqueous extract and its antibacterial activity. *International journal of biological macromolecules* **2019**, *124*, 148-154.
6. Bibi, S.; Ahmad, A.; Anjum, M. A. R.; Haleem, A.; Siddiq, M.; Shah, S. S.; Al Kahtani, A. J. J. o. E. C. E., Photocatalytic degradation of malachite green and methylene blue over reduced graphene oxide (rGO) based metal oxides (rGO-Fe<sub>3</sub>O<sub>4</sub>/TiO<sub>2</sub>) nanocomposite under UV-visible light irradiation. *Journal of Environmental Chemical Engineering* **2021**, *9* (4), 105580.
7. Chand, K.; Jiao, C.; Lakhan, M. N.; Shah, A. H.; Kumar, V.; Fouad, D. E.; Chandio, M. B.; Maitlo, A. A.; Ahmed, M.; Cao, D. J. C. P. L., Green synthesis, characterization and photocatalytic activity of silver nanoparticles synthesized with *Nigella Sativa* seed extract. *Chemical Physics Letters* **2021**, *763*, 138218
8. Chekir, N.; Benhabiles, O.; Tassalit, D.; Laoufi, N. A.; Bentahar, F. J. D.; Treatment, W., Photocatalytic degradation of methylene blue in aqueous suspensions using TiO<sub>2</sub> and ZnO. *Desalination and Water Treatment* **2016**, *57* (13), 6141-6147.

9. Chu, W.; Ma, C.-W. J. W. r., Quantitative prediction of direct and indirect dye ozonation kinetics. *Water research* **2000**, *34* (12), 3153-3160.
10. Demirbas, A., Agricultural based activated carbons for the removal of dyes from aqueous solutions: a review. *Journal of hazardous materials* **2009**, *167* (1-3), 1-9.
11. Fakhari, S.; Jamzad, M.; Fard, H., Green synthesis of zinc oxide nanoparticles: a comparison. *Green Chemistry Letters and Reviews* **2019**, *12*, 19-24.
12. Fadel, Q.; Al-Mashhedy, L. J. B. I. J., Biosynthesis of silver nanoparticles using peel extract of *Raphanus sativus* L. *Biotechnol Ind J* **2017**, *13* (1), 120.
13. Forgacs, E.; Cserhádi, T.; Oros, G., Removal of synthetic dyes from wastewaters: a review. *Environment International* **2004**, *30* (7), 953-971.
14. Gamba, M.; Asllanaj, E.; Raguindin, P. F.; Glisic, M.; Franco, O. H.; Minder, B.; Bussler, W.; Metzger, B.; Kern, H.; Muka, T. J. T. i. F. S.; Technology, Nutritional and phytochemical characterization of radish (*Raphanus sativus*): A systematic review. *Trends in Food Science & Technology* **2021**, *113*, 205-218.
15. García-Montaña, J.; Domènech, X.; García-Hortal, J. A.; Torrades, F.; Peral, J. J. J. o. h. m., The testing of several biological and chemical coupled treatments for Cibacron Red FN-R azo dye removal. *Journal of hazardous materials* **2008**, *154* (1-3), 484-490.
16. Garibo, D.; Borbón-Nuñez, H. A.; de León, J. N. D.; García Mendoza, E.; Estrada, I.; Toledano-Magaña, Y.; Tiznado, H.; Ovalle-Marroquin, M.; Soto-Ramos, A. G.; Blanco, A. J. S. r., Green synthesis of silver nanoparticles using *Lysiloma acapulcensis* exhibit high-antimicrobial activity. *Scientific reports* **2020**, *10* (1), 1-11.
17. Gole, A.; Dash, C.; Ramakrishnan, V.; Sainkar, S.; Mandale, A.; Rao, M.; Sastry, M. J. L., Pepsin-gold colloid conjugates: preparation, characterization, and enzymatic activity. *Langmuir* **2001**, *17* (5), 1674-1679
18. Gul, S.; Ismail, M.; Khan, M. I.; Khan, S. B.; Asiri, A. M.; Rahman, I. U.; Khan, M. A.; Kamboh, M. A. J. A. P. J. o. T. D., Novel synthesis of silver nanoparticles using melon aqueous extract and evaluation of their feeding deterrent activity against housefly *Musca domestica*. *Asian Pacific Journal of Tropical Disease* **2016**, *6* (4), 311-316.
19. Gupta, V. J. J. o. e. m., Application of low-cost adsorbents for dye removal—a review. *Journal of Environmental Management* **2009**, *90* (8), 2313-2342.
20. Hadei, M.; Mesdaghinia, A.; Nabizadeh, R.; Mahvi, A. H.; Rabbani, S.; Naddafi, K. J. E. S.; Research, P., A comprehensive systematic review of photocatalytic degradation of pesticides using nano TiO<sub>2</sub>. *Environmental Science and Pollution Research* **2021**, *28* (11), 13055-13071.
21. Hamedi, S.; Shojaosadati, S. A. J. P., Rapid and green synthesis of silver nanoparticles using *Diospyros lotus* extract: Evaluation of their biological and catalytic activities. *Polyhedron* **2019**, *171*, 172-180.
22. Irshad, M. A.; Nawaz, R.; Rehman, M. Z. u.; Adrees, M.; Rizwan, M.; Ali, S.; Ahmad, S.; Tasleem, S., Synthesis, characterization and advanced sustainable applications of titanium dioxide nanoparticles: A review. *Ecotoxicology and Environmental Safety* **2021**, *212*, 111978.
23. Jain, A.; Anitha, R.; Rajeshkumar, S. J. R. J. o. P.; Technology, Anti-inflammatory activity of Silver nanoparticles synthesized using Cumin oil. *Research Journal of Pharmacy and Technology* **2019**, *12* (6), 2790-2793.
24. Khasawneh, O. F. S.; Palaniandy, P. J. E. T.; Innovation, Removal of organic pollutants from water by Fe<sub>2</sub>O<sub>3</sub>/TiO<sub>2</sub> based photocatalytic degradation: A review. *Environmental Technology & Innovation* **2021**, *21*, 101230.

25. Lee, J.-K.; Gu, J.-H.; Kim, M.-R.; Chun, H.-S. J. J. o. c. e. o. J., Incineration characteristics of dye sludge in a fluidized bed incinerator. *Journal of chemical engineering of Japan***2001**,*34* (2), 171-175.
26. Mallmann, E. J. J.; Cunha, F. A.; Castro, B. N.; Maciel, A. M.; Menezes, E. A.; Fechine, P. B. A. J. R. d. I. d. M. T. d. S. P., Antifungal activity of silver nanoparticles obtained by green synthesis. *Revista do Instituto de Medicina Tropical de São Paulo***2015**,*57*, 165-167.
27. Miri, A.; Shahraki Vahed, H. O.; Sarani, M. J. R. o. C. I., Biosynthesis of silver nanoparticles and their role in photocatalytic degradation of methylene blue dye. *Research on Chemical Intermediates***2018**,*44* (11), 6907-6915.
28. Nguyen, D. T. C.; Le, H. T.; Nguyen, T. T.; Nguyen, T. T. T.; Bach, L. G.; Nguyen, T. D.; Van Tran, T. J. J. o. H. M., Multifunctional ZnO nanoparticles bio-fabricated from *Canna indica* L. flowers for seed germination, adsorption, and photocatalytic degradation of organic dyes. *Journal of Hazardous Materials***2021**,*420*, 126586.
29. Pacioni, N. L.; Borsarelli, C. D.; Rey, V.; Veglia, A. V., Synthetic routes for the preparation of silver nanoparticles. In *Silver nanoparticle applications*, Springer: 2015; pp 13-46.
30. Prado, A. G.; Miranda, B. S.; Jacintho, G. V. J. S. S., Interaction of indigo carmine dye with silica modified with humic acids at solid/liquid interface. *Surface Science***2003**,*542* (3), 276-282.
31. Salleh, M. A. M.; Mahmoud, D. K.; Karim, W. A. W. A.; Idris, A., Cationic and anionic dye adsorption by agricultural solid wastes: A comprehensive review. *Desalination* **2011**,*280* (1), 1-13.
32. Seerangaraj, V.; Sathiyavimal, S.; Shankar, S. N.; Nandagopal, J. G. T.; Balashanmugam, P.; Al-Misned, F. A.; Shanmugavel, M.; Senthilkumar, P.; Pugazhendhi, A. J. J. o. E. C. E., Cytotoxic effects of silver nanoparticles on *Ruellia tuberosa*: Photocatalytic degradation properties against crystal violet and coomassie brilliant blue. *Journal of Environmental Chemical Engineering***2021**,*9* (2), 105088.
33. Sharma, R. J. M. T. P., Synthesis of *Terminalia bellirica* fruit extract mediated silver nanoparticles and application in photocatalytic degradation of wastewater from textile industries. *Materials Today: Proceedings* **2021**,*44*, 1995-1998.
34. Sharma, R.; Sarkar, A.; Jha, R.; Kumar Sharma, A.; Sharma, D., Sol-gel-mediated synthesis of TiO<sub>2</sub> nanocrystals: Structural, optical, and electrochemical properties. *International Journal of Applied Ceramic Technology* **2020**,*17* (3), 1400-1409.
35. Thi Lan Huong, V.; Nguyen, N. T., Green synthesis, characterization and antibacterial activity of silver nanoparticles using *Sapindus mukorossi* fruit pericarp extract. *Materials Today: Proceedings* **2021**,*42*, 88-93.
36. Vadivelan, V.; Kumar, K. V., Equilibrium, kinetics, mechanism, and process design for the sorption of methylene blue onto rice husk. *Journal of colloid and interface science* **2005**,*286* (1), 90-100.
37. Wang, Y.; Qiang, Z.; Zhu, W.; Yao, W.; Tang, S.; Yang, Z.; Wang, J.; Duan, J.; Ma, C.; Tan, R. J. A. A. N. M., BiPO<sub>4</sub> nanorod/graphene composite heterojunctions for photocatalytic degradation of tetracycline hydrochloride. *ACS Applied Nano Materials***2021**,*4* (9), 8680-8689.
38. Zhang, R.; Ma, Y.; Lan, W.; Sameen, D. E.; Ahmed, S.; Dai, J.; Qin, W.; Li, S.; Liu, Y. J. U. s., Enhanced photocatalytic degradation of organic dyes by ultrasonic-assisted electrospray TiO<sub>2</sub>/graphene oxide on polyacrylonitrile/ $\beta$ -cyclodextrin nanofibrous membranes. *Ultrasonics sonochemistry***2021**,*70*, 105343.